

Contact lines with a 180° contact angle

E. S. Benilov[†] and M. Vynnycky

Mathematics Applications Consortium for Science and Industry, Department of Mathematics and Statistics, University of Limerick, Limerick, Ireland

(Received 14 May 2012; revised 11 October 2012; accepted 13 December 2012;
first published online 8 February 2013)

This work builds on the foundation laid by Benney & Timson (*Stud. Appl. Maths*, vol. 63, 1980, pp. 93–98), who examined the flow near a contact line and showed that, if the contact angle is 180° , the usual contact-line singularity does not arise. Their local analysis, however, does not allow one to determine the velocity of the contact line and their expression for the shape of the free boundary involves undetermined constants. The present paper considers two-dimensional Couette flows with a free boundary, for which the local analysis of Benney & Timson can be complemented by an analysis of the global flow (provided that the slope of the free boundary is small, so the lubrication approximation can be used). We show that the undetermined constants in the solution of Benney & Timson can all be fixed by matching the local and global solutions. The latter also determines the contact line's velocity, which we compute among other characteristics of the global flow. The asymptotic model derived is used to examine steady and evolving Couette flows with a free boundary. It is shown that the latter involve brief intermittent periods of rapid acceleration of contact lines.

Key words: contact lines, interfacial flows (free surface), lubrication theory

1. Introduction

It is well known that the Navier–Stokes equations with the standard set of boundary conditions cannot be used if some of the rigid and free boundaries of the flow intersect, resulting in contact lines. This was first shown by Huh & Scriven (1971): treating the shape of the free boundary as given and assuming that it intersects the rigid boundary at a certain contact angle, they demonstrated that the pressure field has a singularity, making the solution physically meaningless. To eliminate the singularity, numerous researchers (e.g. Huh & Scriven 1971; Dussan V. & Davis 1974; Hocking 1976; Hervet & de Gennes 1984; Shikhmurzaev 1993; Wayner 1993; Weidner & Schwartz 1994; Seppacher 1996; Thompson & Troian 1997) replaced the no-slip condition at the rigid boundary with other conditions reflecting various physical models of contact lines.

Note, however, that if the contact angle is 180° , the pressure-field singularity does not arise even if the no-slip condition is imposed on a flow with a contact line.

Two attempts to construct an example of such a flow have been made, by Benney & Timson (1980) and Pismen & Nir (1982). We shall not discuss the latter work in detail, as it contains an error, as pointed out by Ngan & Dussan V. (1984), who also corrected it and showed that the amended solution is meaningless physically (the free

[†] Email address for correspondence: Eugene.Benilov@ul.ie

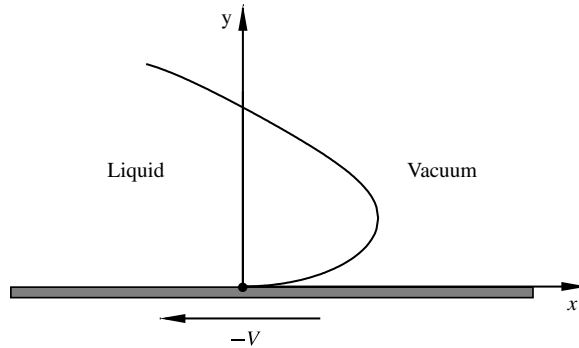


FIGURE 1. The setting of the local analysis by Benney & Timson (1980), in the reference frame co-moving with the contact line (shown by a black dot).

boundary intersects the rigid one twice and approaches the contact line from below the substrate).

Benney & Timson (1980) (hereafter referred to as BT80) considered a two-dimensional flow on a substrate, with the liquid's free boundary and contact line steadily advancing with a velocity V . Given the absence of gravity, the flow is fully characterized by the capillary number

$$C_a = \frac{\mu V}{\sigma}, \quad (1.1)$$

where μ and σ are the liquid's viscosity and surface tension. Using the co-moving reference frame where the contact line is stationary, while the substrate is moving with the velocity $-V$ (see figure 1), BT80 examined the problem (including the no-slip condition) locally, i.e. expanded the solution in powers of the distance from the contact line. It was shown that the free boundary is described by

$$y \sim ax^q \quad \text{as } x \rightarrow 0^+, \quad (1.2)$$

where the origin of the coordinate system (x, y) is associated with the contact line, the x -axis is parallel to the substrate, a is a positive constant and q satisfies

$$\tan q\pi = -2C_a. \quad (1.3)$$

Note that the original version of (1.3) derived by BT80 contained a sign error, again corrected by Ngan & Dussan V. (1984). This error however, unlike that of Pismen & Nir (1982), did not seem to have far-reaching consequences. In particular, equation (1.3) admits infinitely many roots such that $q > 1$, so that the contact angle is indeed 180° and the corresponding solution for the pressure is finite.

Still, even though the (amended) analysis of BT80 yields an apparently sound solution, Ngan & Dussan V. (1984) insisted that:

'it is our belief that there is something inherently wrong with this local boundary-value problem [considered by BT80]. We strongly expect that the solution for the interface shape... is completely determined upon specifying the... contact angle. However, the approach of Benney and Timson does not have this basic characteristic because of the fact that, regardless of the choice of q [in equation (1.2)], the value of the constant a ... remains undetermined.'

Note that, regardless of the above mathematical issue, flows with a 180° contact angle do arise in applications. Indeed, the experiments of Richard & Quéré (1999), Reznik & Yarin (2002) and Aussillous & Quéré (2004) show that, if surface tension is sufficiently strong, drops rolling on a rigid substrate can indeed exhibit contact angles close, or even equal, to 180° . Furthermore, Mahadevan & Pomeau (1999) argued that, for such drops, the pressure singularity is alleviated.

Another example can be seen in gravity waves travelling up a sloping substrate, mostly studied in the context of a tsunami (see Didenkulova *et al.* (2007), Fujima (2007) and Madsen & Fuhrman (2007) and references therein). Given the large-scale of the flow, it has been so far examined only under the approximation of ideal fluid, which ignores the viscous boundary layer near the substrate and, thus, all effects associated with the contact line. Yet the results obtained are in a good agreement with experiments, including the measurements of the run-up distance, which effectively means that the contact line is driven by the macroscopic flow. Most importantly, this can occur only if the contact angle is 180° , otherwise the microscopic flow near the contact line would be singular and, thus, would influence the global dynamics.

It should furthermore be stressed that 180° is not just one of the many allowable values of the contact angle, but a special one, arising in many cases naturally and regardless of the model chosen to describe the contact line.

Consider, for example, the ‘classical’ model, based on the no-slip boundary condition. If the contact angle in this case is not 180° , the contact line cannot move, but the flow still pushes the free boundary, tilting it forward until it ‘overhangs’ the contact line. Eventually, gravity makes the free boundary ‘fall’ onto the rigid one. Once the two boundaries are aligned, a 180° contact angle is formed, and the contact line can move forward.

A similar conclusion can be reached if the no-slip condition on the rigid boundary is replaced with any of the commonly used models for the contact line, provided the velocity of the contact line predicted by this model is much smaller than the velocity of the global flow. In this case, the contact line will not be able to ‘keep up’ with the free boundary, causing, again, the latter to fall onto the substrate.

In general, the examples of rolling drops and tsunami suggest that, if a problem involves strong macroscopic forces (such as gravity and surface tension for drops, or gravity and inertia for a tsunami), these can ‘overwhelm’ the microscopic physics associated with the contact line and enforce a contact angle close to 180° .

The aim of the present work is twofold. First, we resolve the argument between BT80 and Ngan & Dussan V. (1984). Using an example (Couette flows with a free boundary) tractable both locally and globally, we demonstrate that the constant a is uniquely determined by matching the former solution to the latter. We also show that the matching determines the choice of the root of (1.3) for q . Together, the local analysis of BT80 and our global analysis provide a fully consistent description of a flow with a 180° contact angle and no singularity. Second, we shall examine the dynamics of Couette flows with a free boundary, which turn out to have some unusual and interesting features.

The structure of this paper is as follows. In §2, we formulate a boundary-value problem for Couette flows with a free boundary and analyse it asymptotically in §3. In §§4 and 5, we present asymptotic solutions describing steady and unsteady Couette flows, respectively.

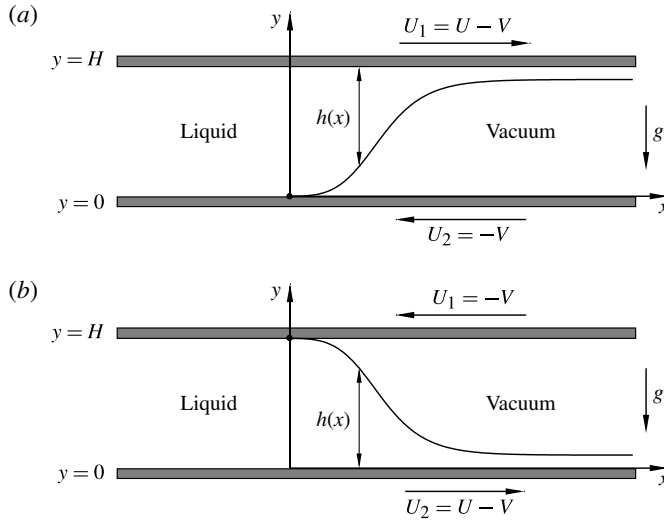


FIGURE 2. Couette flows with a free boundary, in the reference frame co-moving with the contact line: (a) flow of type A; (b) flow of type B.

2. Formulation: a Couette flow with a free boundary

2.1. The governing equations

Consider two horizontal rigid plates separated by a distance H , with the upper and lower plates moving horizontally in opposite directions with velocities U_1 and U_2 (see figure 2). Let the space between the plates, to the left from the free boundary, be filled with an incompressible liquid of density ρ , dynamic viscosity μ and surface tension σ . The density of the gas filling the space to the right from the free boundary will be neglected, i.e. effectively, the gas will be replaced with vacuum. In this work, we confine ourselves to flows depending on two spatial coordinates (x, y) , with the x -axis directed along the lower plate and the y -axis, vertically. We also introduce the time variable t .

Two types of Couette flows with a free boundary will be distinguished:

- (a) type A, where the upper plate is moving to the *right* ($U_1 > 0$) and the lower plate is moving to the *left* ($U_2 < 0$);
- (b) type B, where the velocities are directed the other way around ($U_1 < 0, U_2 > 0$).

In general, the free surface of the liquid-filled region would have contact lines on both plates, but, to simplify the problem, we assume that one of the contact lines is located at infinity. For type A, it is the upper contact line that is at infinity and there is a semi-infinite layer of uniform depth extending to the right (see figure 2a). For flows of type B, in turn, the lower contact line is at infinity, so the semi-infinite layer is on the lower plate also (see figure 2b).

To understand the difference between the two types of Couette flows, observe that, geometrically, one of them can be transformed into the other by interchanging the upper and lower plates. Thus, type A and type B flows differ, essentially, by the direction of gravity.

In what follows, mathematical details will only be discussed in applications to flows of type A, with physics-related issues discussed for both types.

In order to make the contact line stationary, we assume that the velocity of the lower plate matches that of the contact line, i.e.

$$U_1 = U - V, \quad U_2 = -V, \tag{2.1}$$

where V is the velocity of the contact line and U is the velocity of the upper plate relative to the lower plate. Now, we can assume that the contact line is located at $x = 0$. We emphasize that V is an unknown and, thus, is to be solved for, whereas U should be treated as a given parameter. In this work, we assume that U is independent of t , but V , generally, evolves, as does the rest of the flow.

The shape of the free boundary is then described by $y = H - h(x, t)$, where h is the thickness of liquid-filled region (see figure 2a). The flow is described by the stream function ψ and pressure p .

The problem at hand is governed by two non-dimensional parameters. The straightforward choice for these would be the Bond number and C_a (given by (1.1)), but a more convenient one is

$$\varepsilon = \frac{\mu U}{\rho g H^2}, \quad \alpha = \frac{\mu U}{\rho g H^2} \left(\frac{\sigma}{\mu U} \right)^{1/3}, \tag{2.2}$$

where g is the acceleration due to gravity. Physically, ε is the ratio of the viscous force to gravity and α characterizes surface tension.

We shall use the following non-dimensional variables (marked with asterisks):

$$x_* = \frac{x}{H}, \quad y_* = \frac{y}{H}, \quad t_* = \frac{\mu U^2 t}{\rho g H^2}, \tag{2.3}$$

$$\psi_* = \frac{\psi}{UH}, \quad p_* = \frac{p}{\rho g H}, \quad h_* = \frac{h}{H}, \quad V_* = \frac{V}{U}. \tag{2.4}$$

Assuming that the Reynolds number is small, we shall describe the flow by the Stokes equations (asterisks hereinafter omitted):

$$\frac{\partial p}{\partial x} = -\varepsilon \frac{\partial}{\partial y} \left(\frac{\partial^2 \psi}{\partial x^2} + \frac{\partial^2 \psi}{\partial y^2} \right), \quad \frac{\partial p}{\partial y} = -1 + \varepsilon \frac{\partial}{\partial x} \left(\frac{\partial^2 \psi}{\partial x^2} + \frac{\partial^2 \psi}{\partial y^2} \right). \tag{2.5}$$

The no-slip/no-normal-flow conditions at the rigid boundaries are

$$\left. \begin{aligned} \psi = 0, \quad -\frac{\partial \psi}{\partial y} = -V \quad &\text{if } y = 0, x < 0, \\ \psi = -F, \quad -\frac{\partial \psi}{\partial y} = 1 - V \quad &\text{if } y = 1, \end{aligned} \right\} \tag{2.6}$$

where F is the non-dimensional flux of liquid in the x -direction (since the liquid is incompressible, it is constant for $x < 0$). We assume that, as $x \rightarrow -\infty$, the flow becomes homogeneous with respect to x , with zero pressure gradient, which reduces (2.5) to a trivial set of ordinary differential equations with respect to y . Solving them with the boundary conditions (2.6), we obtain

$$F = \frac{1}{2} - V, \tag{2.7}$$

and a quadratic expression for ψ (i.e. as $x \rightarrow -\infty$, the flow has a linear velocity profile).

At the free boundary, mass conservation implies

$$\varepsilon \frac{\partial h}{\partial t} + \frac{\partial}{\partial x} (\psi_{y=1-h}) = 0 \quad \text{if } x > 0, \tag{2.8}$$

and we also require zero tangential stress and relate the normal stress to the curvature of the boundary,

$$\boldsymbol{\tau}^T \mathbf{S} \mathbf{n} = 0, \quad \mathbf{n}^T \mathbf{S} \mathbf{n} = -\frac{\alpha^3 c}{\varepsilon^3} \quad \text{if } y = 1 - h, \ x > 0, \tag{2.9}$$

where

$$\mathbf{n} = \frac{1}{\sqrt{1 + \left(\frac{\partial h}{\partial x}\right)^2}} \begin{bmatrix} \frac{\partial h}{\partial x} \\ 1 \end{bmatrix}, \quad \boldsymbol{\tau} = \begin{bmatrix} -1 \\ \frac{\partial h}{\partial x} \end{bmatrix} \tag{2.10}$$

are the unit normal vector and a tangent vector (not necessarily unit) to the free surface, the superscript ^T denotes matrix transposition,

$$\mathbf{S} = \begin{bmatrix} -2 \frac{\partial^2 \psi}{\partial x \partial y} - \frac{p}{\varepsilon} & \frac{\partial^2 \psi}{\partial x^2} - \frac{\partial^2 \psi}{\partial y^2} \\ \frac{\partial^2 \psi}{\partial x^2} - \frac{\partial^2 \psi}{\partial y^2} & 2 \frac{\partial^2 \psi}{\partial x \partial y} - \frac{p}{\varepsilon} \end{bmatrix} \tag{2.11}$$

is the stress tensor and

$$c = -\frac{\frac{\partial^2 h}{\partial x^2}}{\left[1 + \left(\frac{\partial h}{\partial x}\right)^2\right]^{3/2}} \tag{2.12}$$

is the curvature of the free boundary.

The two scalar conditions (2.9) can be rewritten in the form of a single vector condition,

$$\left(\mathbf{S} + \frac{\alpha^3 c}{\varepsilon^3} \mathbf{I}\right) \mathbf{n} = \mathbf{0} \quad \text{at } y = 1 - h, \ x > 0, \tag{2.13}$$

where \mathbf{I} is the unit matrix. Substituting (2.10)–(2.11) into (2.13), we obtain

$$\left. \begin{aligned} \left(-2 \frac{\partial^2 \psi}{\partial x \partial y} - \frac{p}{\varepsilon} + \frac{\alpha^3 c}{\varepsilon^3}\right) \frac{\partial h}{\partial x} + \frac{\partial^2 \psi}{\partial x^2} - \frac{\partial^2 \psi}{\partial y^2} &= 0, \\ \left(\frac{\partial^2 \psi}{\partial x^2} - \frac{\partial^2 \psi}{\partial y^2}\right) \frac{\partial h}{\partial x} + 2 \frac{\partial^2 \psi}{\partial x \partial y} - \frac{p}{\varepsilon} + \frac{\alpha^3 c}{\varepsilon^3} &= 0, \end{aligned} \right\} \quad \text{if } y = 1 - h, \ x > 0. \tag{2.14}$$

In the next subsection, we shall outline how the boundary-value problem (2.5)–(2.8), (2.12), (2.14) can be analysed asymptotically.

2.2. The set-up of the asymptotic solution

To understand the main difficulty of exploring the global dynamics of flows with a 180° contact angle, observe in figure 1 the point where the tangent to the free surface

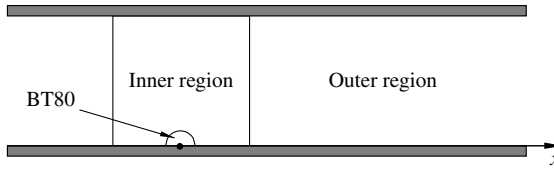


FIGURE 3. A schematic illustrating the asymptotic structure of the solution: the outer ($x \gg 1$) and inner ($x \sim 1$) regions. The local solution of Benney & Timson (1980) represents the $x \ll 1$ limit of the inner region.

is vertical and, thus, the slope is infinite. Such points hamper the (asymptotic) analysis of the global flow, restricting one to local analyses near the contact line.

The Couette flow introduced above is different in this respect, as its free boundary does not involve points of infinite slope. Furthermore, there exists a limit where its slope is small, which enables one to examine the problem through the lubrication approximation.

Indeed, consider the limit

$$\varepsilon \rightarrow 0, \quad \alpha = O(1), \tag{2.15}$$

where the former condition implies that gravity dominates viscosity. It turns out that, subject to (2.15), the slope of the free boundary of the Couette flow can be assumed small (proportional to ε), i.e.

$$h = h(X, t), \tag{2.16}$$

where

$$X = \varepsilon x. \tag{2.17}$$

In what follows, the asymptotic representation (2.16)–(2.17) will be verified by obtaining a consistent asymptotic solution.

It will also be verified that h varies slowly far from, and also near, the contact line, whereas ψ and p do so only in the *outer* region where the distance from the contact line exceeds the width of the channel by an order of magnitude, i.e. $x \gg 1$ (see a schematic in figure 3). The *inner* region, $x = O(1)$, should be examined separately.

With regards to the local solution of BT80, it represents the $x \ll 1$ limit of the inner region. Note, however, that, as follows from (1.1) and (2.2), $C_a = \varepsilon^3/\alpha^3$; hence, equation (2.15) implies

$$C_a \ll 1. \tag{2.18}$$

Thus, to compare our results to those of BT80, the latter should be adapted to small C_a . In particular, equation (1.3) yields

$$q = n - \frac{2C_a}{\pi} + O(C_a^2) \quad \text{as } C_a \rightarrow 0, \tag{2.19}$$

where n is an integer. Since the pressure-field singularity is eliminated only if $q > 1$, it follows that $n \geq 2$. Thus, to leading order in C_a , equation (1.2) yields

$$h = 1 - ax^n + O(x^{n+1}) \quad \text{as } x \rightarrow 0^+. \tag{2.20}$$

It will turn out that matching of the inner and outer solutions is possible only if $n = 2$.

3. The asymptotic analysis

In this section, we shall derive an asymptotic equation for Couette flows of type A. Type B will be briefly discussed in the end of § 3.3.

We shall seek the solution of (2.5)–(2.8), (2.12) and (2.14) in the form

$$\psi = \psi^{(0)} + \varepsilon\psi^{(1)} + \dots, \quad p = p^{(0)} + \varepsilon p^{(1)} + \dots, \tag{3.1a}$$

$$h = h^{(0)} + \varepsilon h^{(1)} + \dots, \quad V = V^{(0)} + \varepsilon V^{(1)} + \dots. \tag{3.1b}$$

Observe that the capillary term in (2.14) appears to exceed all other terms, which would make our perturbation expansion inconsistent. This can be remedied by assuming that

$$h^{(0)} = 1, \quad h^{(1)} = 0, \tag{3.2}$$

in which case (2.12) yields $c = O(\varepsilon^2)$ and the capillary term in (2.14) is ‘balanced’ by the pressure.

In view of a somewhat technical nature of this section, readers interested mostly in the physical aspects of the problem at hand are advised to skip to § 3.3.

3.1. The inner region

3.1.1. The leading-order equations

To leading-order, the boundary-value problem (2.5)–(2.8), (2.12), (2.14) yields

$$\frac{\partial p^{(0)}}{\partial x} = 0, \quad \frac{\partial p^{(0)}}{\partial y} = -1, \tag{3.3}$$

$$\left. \begin{aligned} \psi^{(0)} = 0, \quad \frac{\partial \psi^{(0)}}{\partial y} = V^{(0)} \quad &\text{if } y = 0, \ x < 0, \\ \psi^{(0)} = 0 \quad \frac{\partial^2 \psi^{(0)}}{\partial y^2} = 0 \quad &\text{if } y = 0, \ x > 0, \end{aligned} \right\} \tag{3.4}$$

$$\psi^{(0)} = -\frac{1}{2} + V^{(0)}, \quad -\frac{\partial \psi^{(0)}}{\partial y} = 1 - V^{(0)} \quad \text{if } y = 1, \tag{3.5}$$

$$-p^{(0)} - \alpha^3 \frac{\partial^2 h^{(2)}}{\partial x^2} = 0 \quad \text{if } y = 0, \ x > 0 \tag{3.6}$$

(observe that, to leading-order, the free boundary has to be moved from $y = 1 - h$ to $y = 0$).

Now, it follows from (3.3) and (3.6) that

$$p^{(0)} = b_1 - y, \tag{3.7}$$

$$h^{(2)} = -\frac{b_1}{2\alpha^3}x^2 + b_2x, \tag{3.8}$$

where b_1 and b_2 are order-one constants, and it has been taken into account that $(h)_{x=0} = 1$, hence, $(h^{(2)})_{x=0} = 0$. The constants b_1 and b_2 will be found through the inner-to-outer matching and the requirement that the higher-order inner solution be regular, respectively.

3.1.2. The boundary-value problem for $\psi^{(0)}$

Observe that the zeroth-order equations (3.3)–(3.6) leave $\psi^{(0)}$ undetermined, which can be remedied by considering the first order of the Stokes equations (2.5),

$$\frac{\partial p^{(1)}}{\partial x} = -\frac{\partial}{\partial y} \left(\frac{\partial^2 \psi^{(0)}}{\partial x^2} + \frac{\partial^2 \psi^{(0)}}{\partial y^2} \right), \quad \frac{\partial p^{(1)}}{\partial y} = \frac{\partial}{\partial x} \left(\frac{\partial^2 \psi^{(0)}}{\partial x^2} + \frac{\partial^2 \psi^{(0)}}{\partial y^2} \right) \tag{3.9}$$

(the rest of the other first-order equations will not be needed). Eliminating $p^{(1)}$ by ‘cross-differentiation’, one can readily obtain the usual biharmonic equation for $\psi^{(0)}$,

$$\left(\frac{\partial^2}{\partial x^2} + \frac{\partial^2}{\partial y^2}\right) \left(\frac{\partial^2 \psi^{(0)}}{\partial x^2} + \frac{\partial^2 \psi^{(0)}}{\partial y^2}\right) = 0. \tag{3.10}$$

This equation and the boundary conditions (3.4)–(3.5) fully determine $\psi^{(0)}$. In particular, one can show that

$$\psi^{(0)} \rightarrow -\frac{1}{4}y^3 + (V^{(0)} - \frac{1}{4})y \quad \text{as } x \rightarrow +\infty. \tag{3.11}$$

Note that, treating (3.10), (3.4)–(3.5) as a particular case of the boundary-value problem considered by Moffatt (1964), it can be verified that its solution is such that $p^{(1)}$ in (3.9) does not involve a singularity (which it would do, should the contact angle be anything but 180°).

To be specific, an explicit solution of (3.10) can be sought in the form of a series in half-integer powers of the radial variable $r = (x^2 + y^2)^{1/2}$,

$$\psi^{(0)} = \sum_{n=0}^{\infty} r^n \left[f_n^{(0)}(\phi) + r^{1/2} f_{n+1/2}^{(0)}(\phi) \right], \tag{3.12}$$

where ϕ is the polar angle, and the functions $f_\gamma^{(0)}$ satisfy

$$\left[(\gamma - 2)^2 + \frac{\partial^2}{\partial \phi^2} \right] \left(\gamma^2 f_\gamma^{(0)} + \frac{\partial^2 f_\gamma^{(0)}}{\partial \phi^2} \right) = 0. \tag{3.13}$$

This ordinary differential equation can be readily solved. Imposing the boundary conditions (3.4) and requiring that $p^{(1)}$ in (3.9) be regular (which requires $f_0 = f_{1/2} = f_{3/2} = 0$), one can obtain

$$\begin{aligned} \psi^{(0)} = & rV^{(0)} \sin \phi + \frac{2}{5} r^{5/2} A_{5/2}^{(0)} \left(\sin \frac{5}{2} \phi - \sin \frac{1}{2} \phi \right) \\ & + \sum_{n=3}^{\infty} \left\{ r^n A_n^{(0)} \left[\frac{\sin n\phi}{n} - \frac{\sin(n-2)\phi}{n-2} \right] \right. \\ & \left. + r^{n+1/2} A_{n+1/2}^{(0)} \frac{\sin \left(n + \frac{1}{2} \right) \phi - \sin \left(n - \frac{3}{2} \right) \phi}{n + \frac{1}{2}} \right\}, \end{aligned} \tag{3.14}$$

where the coefficients $A_\gamma^{(0)}$ can, in principle, be determined from the boundary condition (3.5).

3.1.3. The boundary-value problem for $\psi^{(2)}$

It turns out that, to determine the constant b_2 in expression (3.8), one needs to examine the behaviour of $\psi^{(2)}$. The corresponding boundary-value problem can be extracted from the second and third orders of the exact equations (2.5)–(2.8), (2.12) and (2.14), which yield

$$\left(\frac{\partial^2}{\partial x^2} + \frac{\partial^2}{\partial y^2}\right) \left(\frac{\partial^2 \psi^{(2)}}{\partial x^2} + \frac{\partial^2 \psi^{(2)}}{\partial y^2}\right) = 0, \tag{3.15}$$

$$\psi^{(2)} = 0, \quad \frac{\partial \psi^{(2)}}{\partial y} = V^{(2)} \quad \text{if } y = 0, \ x < 0, \tag{3.16}$$

$$\psi^{(2)} - \frac{\partial \psi^{(0)}}{\partial y} h^{(2)} = 0 \quad \text{if } y = 0, \ x > 0, \tag{3.17}$$

$$4 \frac{\partial^2 \psi^{(0)}}{\partial x \partial y} \frac{\partial h^{(2)}}{\partial x} - \frac{\partial^2 \psi^{(2)}}{\partial x^2} + \frac{\partial^2 \psi^{(2)}}{\partial y^2} + \left(\frac{\partial^3 \psi^{(0)}}{\partial x^2 \partial y} - \frac{\partial^3 \psi^{(0)}}{\partial y^3} \right) h^{(2)} = 0 \quad \text{if } y = 0, \ x > 0, \tag{3.18}$$

$$\frac{\partial \psi^{(2)}}{\partial y} = V^{(2)}, \quad \psi^{(2)} = 0 \quad \text{if } y = 1. \tag{3.19}$$

Substituting expressions (3.8) and (3.14) for $h^{(2)}$ and $\psi^{(0)}$ into (3.15)–(3.18), one can demonstrate that

$$\psi^{(2)} = r \left[V^{(0)} b_2 \cos \phi + \left(V^{(2)} + \frac{V^{(0)} b_2}{\pi} \right) \sin \phi - \frac{V^{(0)} b_2}{\pi} \phi \cos \phi \right] + O(r^2). \tag{3.20}$$

It can then be shown that, unless $b_2 = 0$, the last term in the square brackets in the above expression makes the higher-order pressure $p^{(3)}$ singular. Thus, equation (3.8) yields

$$h^{(2)} = -\frac{b_1}{2\alpha^3} x^2. \tag{3.21}$$

This equality implies that the small- X behaviour of the assumed outer solution (2.16)–(2.17) is

$$h(X, t) = 1 - \frac{b_1}{2\alpha^3} X^2 + O(\varepsilon) \quad \text{as } X \rightarrow 0^+. \tag{3.22}$$

This equality will be used as a boundary condition for the outer solution in the next section.

3.2. The outer problem

The outer region can be examined using the standard lubrication approximation, based on the small-slope assumption (2.16)–(2.17).

Since we do not need to delve into the perturbation expansion deeper than the leading order, we shall not expand the unknowns, but simply rewrite the boundary-value problem (2.5)–(2.8), (2.12) and (2.14) in terms of (X, y) , omit all small terms and replace $V \rightarrow V^{(0)}$,

$$\frac{\partial p}{\partial X} = -\frac{\partial^3 \psi}{\partial y^3}, \quad \frac{\partial p}{\partial y} = -1, \tag{3.23}$$

$$\left. \begin{aligned} \psi &= 0, & -\frac{\partial \psi}{\partial y} &= -V^{(0)} & \text{if } y = 0, \ X < 0, \\ \psi &= V^{(0)} - \frac{1}{2}, & -\frac{\partial \psi}{\partial y} &= 1 - V^{(0)} & \text{if } y = 1, \end{aligned} \right\} \tag{3.24}$$

$$\frac{\partial h}{\partial t} + \frac{\partial}{\partial X} (\psi_{y=1-h}) = 0 \quad \text{if } X > 0, \tag{3.25}$$

$$\left. \begin{aligned} \frac{\partial^2 \psi}{\partial y^2} &= 0 \\ -p - \alpha^3 \frac{\partial^2 h}{\partial X^2} &= 0 \end{aligned} \right\} \text{ if } y = 1 - h, X > 0. \tag{3.26}$$

For negative X , these equations yield

$$\psi = -\frac{1}{2}y^2 + V^{(0)}y \quad \text{if } X < 0, \tag{3.27}$$

which corresponds to a linear velocity profile (as it should do in a Couette flow without free boundary). For positive X , following the usual routine of the lubrication approximation, one can use (3.23)–(3.26) to deduce

$$\begin{aligned} \psi = & - \left(\alpha^3 \frac{\partial^3 h}{\partial X^3} + \frac{\partial h}{\partial X} \right) \frac{(1-y)^3}{6} + h \left(\alpha^3 \frac{\partial^3 h}{\partial X^3} + \frac{\partial h}{\partial X} \right) \frac{(1-y)^2}{2} \\ & + (1 - V^{(0)}) (1-y) - \frac{1}{2} + V^{(0)}, \end{aligned} \tag{3.28}$$

$$\frac{\partial h}{\partial t} + \frac{\partial}{\partial X} \left[\frac{h^3}{3} \left(\alpha^3 \frac{\partial^3 h}{\partial X^3} + \frac{\partial h}{\partial X} \right) + (1 - V^{(0)}) h \right] = 0. \tag{3.29}$$

To match h to the inner solution (3.22), one must require

$$h = 1 \quad \text{if } X = 0, \tag{3.30}$$

$$\frac{\partial h}{\partial X} = 0 \quad \text{if } X = 0. \tag{3.31}$$

Next, matching the outer expression (3.28) to the limiting expression (3.11) of the inner solution and taking into account (3.30)–(3.31), we obtain

$$\frac{\partial^3 h}{\partial X^3} = -\frac{3}{2\alpha^3} \quad \text{if } X = 0. \tag{3.32}$$

We shall also require that

$$\frac{\partial h}{\partial X} \rightarrow 0 \quad \text{as } X \rightarrow +\infty, \tag{3.33}$$

which reflects the geometry of type A flows at plus infinity (see figure 2a).

As we shall see below, the boundary-value problem (3.29)–(3.33) determines both $h(X, t)$ and $V^{(0)}(t)$.

3.3. Discussion

(i) Physically, the boundary condition (3.30) implies that the free surface becomes ‘attached’ to the substrate at $X = 0$. Condition (3.31), in turn, makes the contact angle be 180°.

In order to understand the physical meaning of condition (3.32), observe that, using (3.30)–(3.31), it can be rewritten in the form

$$\frac{h^3}{3} \left(\alpha^3 \frac{\partial^3 h}{\partial X^3} + \frac{\partial h}{\partial X} \right) + (1 - V^{(0)}) h = \frac{1}{2} - V^{(0)} \quad \text{if } X = 0. \tag{3.34}$$

The left-hand side of this equality represents the horizontal component of the non-dimensional flux, whereas the right-hand side is the flux at $X < 0$. Thus, equation (3.32) is simply a condition that the flux be continuous.

(ii) It is instructive to consider the right-hand half ($X > 0$) of the flow separately and interpret it as a flow of a liquid film injected at $X = 0$ onto a plate moving with a given velocity $V^{(0)}$. In this case, only two boundary conditions at the injection point are needed, prescribing the film thickness and the flux. In the present problem, however, there is also the condition for the contact angle, but, on the other hand, $V^{(0)}$ is unknown.

Thus, condition (3.31) that the contact angle be 180° determines, in a sense, the velocity of the contact line.

(iii) We shall also explain how one can fix the constant a in expression (1.2) (this issue is important since the criticism of Ngan & Dussan V. (1984) was based on the fact that, in the local analysis of BT80, a remained undetermined). To do so, observe that the comparison of expression (3.22) with the $C_a \rightarrow 0$ asymptotics of the BT80 solution (2.20) and (2.19) yields

$$n = 2, \quad (3.35)$$

$$a = \frac{1}{2} \varepsilon^2 \left(\frac{\partial^2 h}{\partial^2 X} \right)_{X=0}. \quad (3.36)$$

Equality (3.36) demonstrates that a is determined by the outer solution, whereas the former equality fixes the constant q (which appears in solution (1.2) and (2.19) of BT80).

(iv) The asymptotic boundary-value problem for flows of type B is similar to the type A problem (3.29)–(3.31). In fact, the boundary conditions are exactly the same as (3.30)–(3.31), whereas the governing equation for type-B flows is

$$\frac{\partial h}{\partial t} + \frac{\partial}{\partial X} \left[\frac{h^3}{3} \left(\alpha^3 \frac{\partial^3 h}{\partial X^3} - \frac{\partial h}{\partial X} \right) + (1 - V^{(0)}) h \right] = 0, \quad (3.37)$$

which differs from (3.29) only by the minus in front of the term involving $\partial h / \partial X$. The difference is due to the fact that the term in question originates from the hydrostatic pressure gradient in the Stokes equations. Then, since in type A and type B flows the liquid clings to the upper and lower plates, respectively, gravity affects them in opposite ways.

4. Steady Couette flows

In what follows, we shall omit the superscript (0) from V and, thus, write (3.29) and (3.37) in the form

$$\frac{\partial h}{\partial t} + \frac{\partial}{\partial X} \left[\frac{h^3}{3} \left(\alpha^3 \frac{\partial^3 h}{\partial X^3} + \frac{\partial h}{\partial X} \right) + (1 - V) h \right] = 0 \quad (\text{type A}), \quad (4.1)$$

and

$$\frac{\partial h}{\partial t} + \frac{\partial}{\partial X} \left[\frac{h^3}{3} \left(\alpha^3 \frac{\partial^3 h}{\partial X^3} - \frac{\partial h}{\partial X} \right) + (1 - V) h \right] = 0 \quad (\text{type B}). \quad (4.2)$$

In this section, we examine steady solutions of the boundary-value problems (4.1), (3.30)–(3.33) and (4.2), (3.30)–(3.33).

4.1. Couette flows of type A

Assuming that h does not depend on t , integrating (4.1) with respect to X , and eliminating the constant of integration using the boundary conditions (3.30)–(3.32),

we obtain

$$\frac{1}{3}h^3 (\alpha^3 h''' + h') + (1 - V)h = \frac{1}{2} - V, \tag{4.3}$$

$$h = 1, \quad h' = 0 \quad \text{if } X = 0, \tag{4.4}$$

$$h' \rightarrow 0 \quad \text{as } X \rightarrow +\infty, \tag{4.5}$$

where the prime denotes differentiation with respect to X .

It is instructive to compare the boundary-value problem (4.3)–(4.5) with the so-called ‘drag-out problem’ examined by Landau & Levich (1942). By comparison with the Landau–Levich equation, equation (4.3) includes an extra term h' describing gravity, but, mathematically, this difference is not essential. The main difference between the two problems results from the extra boundary condition in (4.4).

To understand why a *third*-order ordinary differential equation (ODE) (4.3) and *three* boundary conditions (4.4)–(4.5) fix both h and V , observe that (4.3) and (4.5) are consistent only if

$$h \rightarrow \frac{\frac{1}{2} - V}{1 - V} \quad \text{as } X \rightarrow +\infty. \tag{4.6}$$

Physically, the limiting value of h should be positive and less than unity (otherwise the free boundary would pass through the walls of the channel), which implies

$$V \leq \frac{1}{2}. \tag{4.7}$$

To examine the behaviour of h as $X \rightarrow +\infty$, rewrite (4.3) and (4.6) in terms of

$$\hat{h} = h - \frac{\frac{1}{2} - V}{1 - V}, \tag{4.8}$$

linearize (4.3) and obtain

$$\alpha^3 \hat{h}''' + \hat{h}' + \frac{3(1 - V)^4}{(\frac{1}{2} - V)^3} \hat{h} = 0, \tag{4.9}$$

$$\hat{h} \rightarrow 0 \quad \text{as } X \rightarrow +\infty. \tag{4.10}$$

The solution of this boundary-value problem is

$$\hat{h} = A_1 e^{\lambda_1 X} + A_2 e^{\lambda_2 X} + A_3 e^{\lambda_3 X}, \tag{4.11}$$

where $A_{1,2,3}$ are undetermined constants and $\lambda_{1,2,3}$ satisfy

$$\alpha^3 \lambda^3 + \lambda + \frac{3(1 - V)^4}{(\frac{1}{2} - V)^3} = 0, \tag{4.12}$$

$$\text{Re } \lambda < 0. \tag{4.13}$$

Without loss of generality, it can be assumed

$$\text{Im } \lambda_1 = 0, \quad \lambda_2 = \lambda_3^*. \tag{4.14}$$

Then, given (4.7),

$$\lambda_1 < 0, \tag{4.15}$$

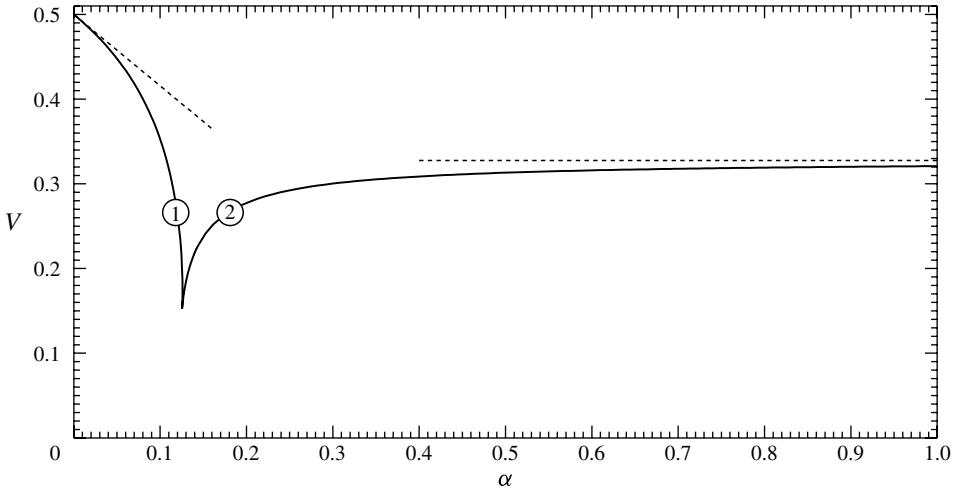


FIGURE 4. The dependence of the contact line’s velocity V on the parameter α as determined by the boundary-value problem (4.6)–(4.11). The dotted lines show the asymptotic solutions (A 1), (A 12) ($\alpha \rightarrow 0$) and (A 24) ($\alpha \rightarrow \infty$). The solutions $h(X)$ corresponding to points 1 and 2 are shown in figure 5.

i.e. λ_1 does satisfy (4.13). To show that $\lambda_{2,3}$ do not, apply the Vieta formula to (4.12), which yields

$$\lambda_1 + \lambda_2 + \lambda_3 = 0. \tag{4.16}$$

Together with (4.14)–(4.15), this equality proves that $\lambda_{2,3}$ do not satisfy condition (4.13).

Omitting, thus, the terms involving $A_{2,3}$ from solution (4.11) and (4.8), we obtain

$$h \sim \frac{\frac{1}{2} - V}{1 - V} + A_1 e^{\lambda_1 X} \quad \text{as } X \rightarrow +\infty. \tag{4.17}$$

Most importantly, this asymptotic includes only one free constant, A_1 , which makes it impossible for a solution satisfying (4.17) to also satisfy two conditions (4.4) at $X = 0$.

Thus, to satisfy all of the boundary conditions, V must also be adjusted, i.e. it should be treated as an eigenvalue (which is not unusual for problems with contact lines; see, for example, Hocking (1977)).

The boundary-value problem (4.3)–(4.5) was solved asymptotically for the limits of small and large α (see appendix A), with the general case examined numerically by shooting. The most important characteristic of the solution, the dependence of the velocity V of the contact line on the capillary parameter α , is shown in figure 4.

One can see that the curve $V(\alpha)$ involves a cusp located at

$$\alpha_c \approx 0.1255. \tag{4.18}$$

Typical examples of $h(X)$ corresponding to $\alpha < \alpha_c$ and $\alpha > \alpha_c$ are shown in figure 5. Clearly, the latter solutions are meaningless physically, as they describe flows with the free boundary passing through the lower plate.

Thus, meaningful solutions for steady Couette flows with a free boundary exist in a relatively narrow range of α (this conclusion will be discussed in more detail later).

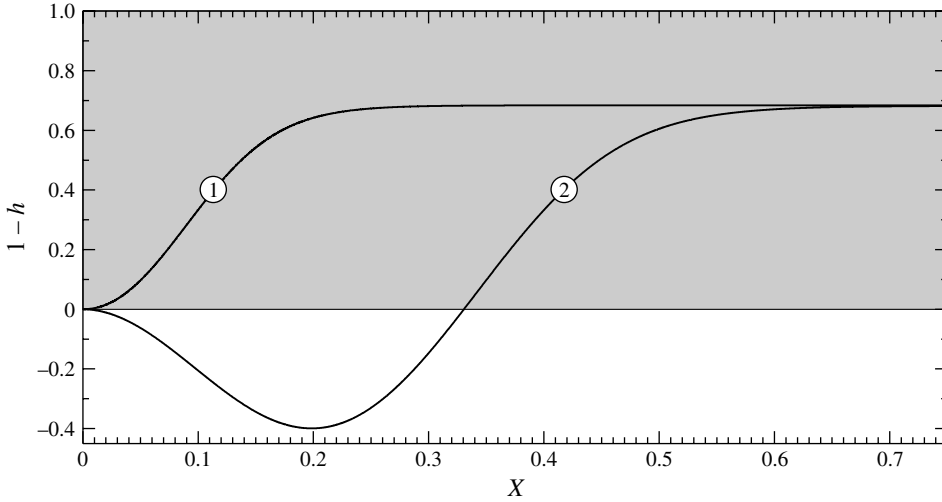


FIGURE 5. Examples of solutions of the boundary-value problem (4.6)–(4.11) corresponding to points indicated in figure 4: (1) $\alpha = 0.1193$; (2) $\alpha = 0.18$. The region inside the channel is shaded. Observe that, in (2), the free boundary passes through the lower plate making this example physically meaningless.

4.2. Couette flows of type B

The type B equivalent of the type A (4.3) is

$$\frac{1}{3}h^3 (\alpha^3 h''' - h') + (1 - V)h = \frac{1}{2} - V. \tag{4.19}$$

The minus in front of h' in (4.19) turns out to be important, as the boundary-value problem (4.19), (4.4)–(4.5) does not admit physically meaningful solutions (such that $0 \leq h \leq 1$) for any value of α . A rigorous proof of this fact can be found in appendix B.

We conclude that Couette flows of type B cannot be steady.

4.3. Discussion

(i) To understand why flows of type B cannot be steady, note that steady solutions usually reflect a balance between some opposing effects, such as nonlinearity and dispersion for solitons or nonlinearity and viscosity for shock waves.

Next, observe that the terms $\partial^3 h / \partial X^3$ and $\partial h / \partial X$ in the type B (4.2) represent the regular and higher-order diffusion, respectively. Both these effects make the solution spread out and, in the absence of an opposing effect, no steady state exists.

In the type A (4.1), in turn, the second derivative represents anti-diffusion (making the solution contract), with the fourth derivative still representing higher-order diffusion (making the solution spread out). The steady states existing in this case can be interpreted as a result of a balance between these two opposing effects of diffusion.

(ii) As mentioned above, steady Couette flows exist only if

$$\alpha \lesssim 0.1255. \tag{4.20}$$

It turns out, however, that this condition is not too restrictive and leaves plenty of room for experimental verification of the results obtained.

Indeed, let the liquid under consideration be water at 20 °C, for which

$$\rho \approx 1.00 \times 10^3 \text{ kg m}^{-3}, \quad \mu \approx 1.01 \times 10^{-3} \text{ Pa s}, \quad \sigma \approx 7.28 \times 10^{-2} \text{ N m}^{-1}. \quad (4.21)$$

Assume also that the height H of the channel and the velocity difference U between the plates are in the range

$$H \geq 1 \text{ mm}, \quad U \leq 15 \text{ cm s}^{-1}. \quad (4.22)$$

Then, ε and α (given by (2.2)) are

$$\varepsilon \lesssim 0.0154, \quad \alpha \lesssim 0.1211, \quad (4.23)$$

i.e. α is inside range (4.20) and ε is small.

Thus, for all of the parameter range (4.21)–(4.22), steady Couette flows of type A exist and our results hold comfortably.

5. Non-steady Couette flows

Since steady solutions do not exist for all type B flows and for some type A flows, these cases will be illustrated with evolving solutions. Those have been obtained numerically, using the finite-element solver available in the COMSOL Multiphysics package.

5.1. Preliminary comments

The main difficulty of simulating the asymptotic models derived is associated with the fact that they both admit solutions such that $V(t)$ ‘explodes’ at a finite time,

$$V \rightarrow -\infty \quad \text{as } t \rightarrow t_e, \quad (5.1)$$

where t_e is the time of the ‘explosion’. The singularity of V is accompanied by a singularity in $\partial h/\partial t$, whereas h remains finite.

In general, solutions developing a singularity in a finite time arise in many physical settings (e.g. Talanov 1964; Zakharov 1972; Bertozzi & Pugh 1996, 2000; Benilov, O’Brien & Sazonov 2003; Benilov 2004, etc.). In application to the problem at hand, the physical implications of the singular behaviour will be discussed in § 5.3, whereas now we shall explain how it was handled numerically.

Since a solution is physically meaningful only until the explosion, the simplest way to simulate it consists of changing the time variable $t \rightarrow T$ in such a way that the time of explosion $t = t_e$ corresponds to $T = \infty$. Furthermore, since t_e depends on the given initial condition and cannot be predicted beforehand, the expression for T may not involve t explicitly, but only through the dependent variables, e.g.

$$T = \int_0^t f(V(\tau)) \, d\tau, \quad (5.2)$$

where the function $f(V) > 0$ is such that the integral in the above expression diverges as $t \rightarrow t_e$.

As nothing was known *a priori* about the nature of the singularity of $V(t)$, $f(V)$ had to be chosen through trial and error. First, several examples of the form $f = 1 + V^{2n}$ were tested, but, no matter how large n was, the explosion still occurred at a finite T (i.e. the integral in (5.2) did not diverge). This indicates that the singularity of $V(t)$ is weaker than algebraic (e.g. logarithmic).

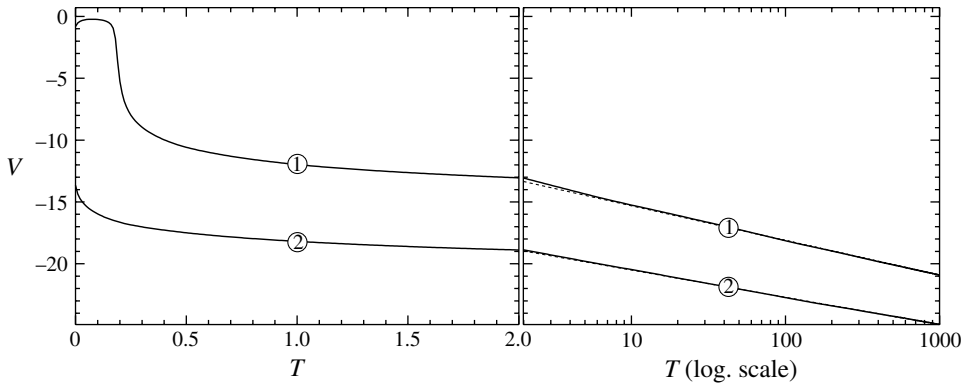


FIGURE 6. The dependence of the velocity V of the contact line versus T (related to the physical time by (5.3)) for the type A problem (5.4), (3.30)–(3.33), with the initial condition such that it would be the steady state at $\alpha = 0.1254$. Curves (1) and (2) represent $\alpha = 0.1357$ and $\alpha = 0.3979$. The left- and right-hand panels show the medium and large T behaviours, respectively. The dotted lines correspond to dependence (5.5) with $c_1 = 2.8$, $c_2 = -12.51$ ($\alpha = 0.1357$) and $c_1 = 2.2$, $c_2 = -18.37$ ($\alpha = 0.3979$).

Eventually, an exponentially growing $f(V)$,

$$T = \int_0^t \{1 + \exp[-V(\tau)]\} d\tau, \tag{5.3}$$

has turned out to be sufficient. In terms of T , equation (4.1), for example, becomes

$$\frac{\partial h}{\partial T} + \frac{1}{1 + e^{-V}} \frac{\partial}{\partial X} \left[\frac{h^3}{3} \left(\alpha^3 \frac{\partial^3 h}{\partial X^3} + \frac{\partial h}{\partial X} \right) + (1 - V)h \right] = 0, \tag{5.4}$$

whereas the boundary conditions (3.30)–(3.33) remain the same as before.

5.2. Numerical results

It was found that, in all cases where steady states exist (i.e. for the type A model with $\alpha \lesssim 0.1255$), the solution would typically evolve towards these states. We conclude that they are stable.

In all other cases, for models of both types, the solutions evolve in such a way that $V(T) \rightarrow -\infty$ as $T \rightarrow \infty$ (see typical examples in figure 6). The long T behaviour of $V(T)$ is well approximated by

$$V(T) \sim -c_1 \ln T + c_2 \quad \text{as } T \rightarrow \infty, \tag{5.5}$$

where c_1 and c_2 are constants. The former is more important, as the corresponding term dominates expression (5.5) as $T \rightarrow \infty$. Our computations show that, typically,

$$2 < c_1 < 3. \tag{5.6}$$

In terms of the physical time t (related to T by (5.3)), expression (5.5) corresponds to an ‘explosion’,

$$V(t) \sim \frac{c_1}{c_1 - 1} \ln(t_e - t) + c_2 \quad \text{as } t \rightarrow \infty, \tag{5.7}$$

where the explosion time t_e is, mathematically, a constant of integration. In what follows, behaviour (5.7) will be referred to as the ‘explosion law’.

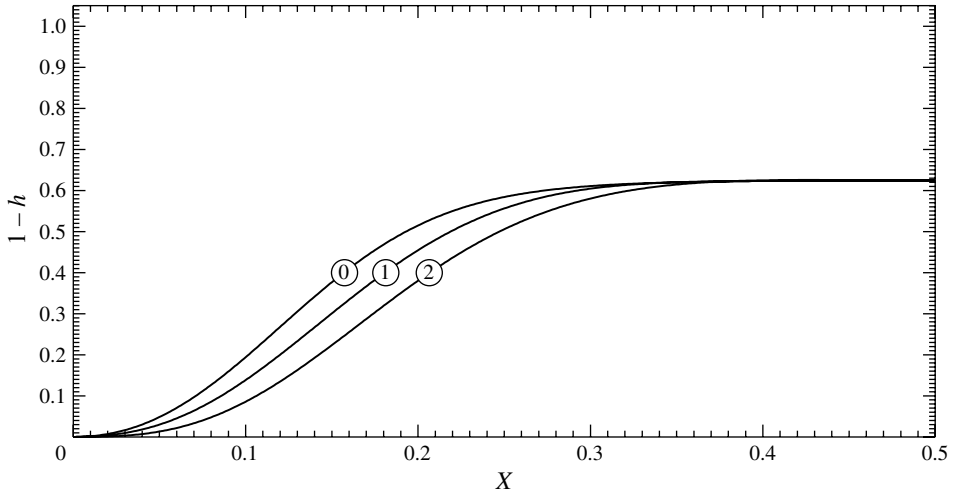


FIGURE 7. The evolution of the solution h versus X for $\alpha = 0.1357$, corresponding to curve (1) in figure 6. Curves (0), (1), (2) correspond to $T = 0, 0.1, 0.2$. The solution for $T > 0.2$ is very close to that for $T = 0.2$.

Interestingly, even though $V(t)$ becomes singular at $t = t_e$, the corresponding solution $h(X, t)$ remains finite and smooth (see figure 7). Another interesting property of solutions with ‘exploding’ $V(t)$ is that no qualitative differences have been observed between the type A and type B models.

These and other qualitative questions will be discussed in the next subsection.

5.3. Discussion

(i) Observe that, as follows from asymptotics (4.7), the singularity of $V(t)$ is integrable, so, even though the velocity of the contact line becomes infinite, its displacement is finite.

It can further be shown (using the results of § 3) that the slope of the free surface and the velocity of liquid particles relative to the plates are both finite at all times. The latter conclusion is best illustrated physically for flows of type B (see figure 1*b*). In this case, a solution with large, negative V corresponds to a rapid, leftward motion of the contact line, which, however, can be achieved through a slow, downward motion of the liquid particles (as if the liquid ‘peels off’ the upper plate). In fact, given the no-slip boundary condition, the downward motion of liquid particles is the only way to make the contact line move horizontally.

Still, even though the liquid’s relative velocity at the time of explosion is finite, its absolute acceleration is not, which violates the validity of the Stokes equations. As a result, exploding solutions lose applicability a short time before the explosion.

On the other hand, they are still applicable during the lead-up to the explosion, suggesting a tendency to spontaneous acceleration of contact lines in Couette flows with a free boundary.

(ii) The counter-intuitive fact that V becomes infinite while h remains finite can be explained by relating the former to the latter. To do so for, say, the type A model, differentiate (4.1) with respect to X , set $X = 0$, and take into account (3.30)–(3.32),

which yields

$$V = \left(\frac{\alpha^3 \frac{\partial^5 h}{\partial X^5} - \frac{1}{2\alpha^3}}{\frac{\partial^2 h}{\partial X^2}} \right)_{X=0} - \frac{1}{2}. \tag{5.8}$$

This expression shows that V can tend to infinity as

$$\frac{\partial^2 h}{\partial X^2} \rightarrow 0, \tag{5.9}$$

with h remaining finite.

A similar conclusion holds for the type B model, as the corresponding expression for V differs from its type A equivalent (5.8) only by the sign of the $1/2\alpha^3$ term. Note also that our computations confirm that the second derivative of h vanishes at the moment of explosion.

(iii) To explain the apparent similarity of the exploding solution for the type A and type B models, we impose for simplicity an additional assumption that

$$h = 1 + \tilde{h}, \quad |\tilde{h}| \ll 1 \tag{5.10}$$

(we emphasize that, until now, we considered the general case, where the variation of h was order one). Linearizing accordingly the type A and type B equations (4.1) and (4.2), we obtain

$$\frac{\partial \tilde{h}}{\partial t} + \frac{1}{3} \left(\alpha^3 \frac{\partial^4 \tilde{h}}{\partial X^4} \pm \frac{\partial^2 \tilde{h}}{\partial X^2} \right) + (1 - V) \frac{\partial \tilde{h}}{\partial X} = 0, \tag{5.11}$$

where the \pm correspond to the types A/B. Next, observe that, if the solution approaches the explosion and, thus,

$$|V| \gg 1, \tag{5.12}$$

the last term in (5.11) can be ‘balanced’ by the other terms only if the spatial and time scales are

$$\Delta X = O(|V|^{-1/3}), \quad \Delta t = O(|V|^{-4/3}). \tag{5.13}$$

This scaling implies that

$$\left| \frac{\partial^4 \tilde{h}}{\partial X^4} \right| \gg \left| \frac{\partial^2 \tilde{h}}{\partial X^2} \right|. \tag{5.14}$$

Taking into account (5.12) and (5.14), one can reduce (5.11) to

$$\frac{\partial \tilde{h}}{\partial t} + \frac{\alpha^3}{3} \frac{\partial^4 \tilde{h}}{\partial X^4} - V \frac{\partial \tilde{h}}{\partial X} = 0. \tag{5.15}$$

Finally, applying assumptions (5.10) and (5.12)–(5.13) to the boundary conditions (3.30)–(3.33) and assuming

$$|\tilde{h}| = O(|V|^{-1}), \tag{5.16}$$

we obtain

$$\tilde{h} = 0, \quad \frac{\partial \tilde{h}}{\partial X} = 0, \quad \frac{\partial^3 \tilde{h}}{\partial X^3} = -\frac{3}{2\alpha^3} \quad \text{if } X = 0, \quad (5.17)$$

$$\frac{\partial \tilde{h}}{\partial X} \rightarrow 0 \quad \text{as } X \rightarrow +\infty. \quad (5.18)$$

Observe that the boundary-value problem (5.15)–(5.18) is the same for the models of both types. Given that, as $|V| \rightarrow \infty$, the validity of (5.15) only improves, one can see why the exploding solutions of the two types are alike.

The above argument, however, holds only under assumption (5.10). For solutions such that (5.10) does not hold, one can conjecture that the explosion law (5.7) is determined by a narrow region near the contact line and arrive to the same conclusion.

The boundary-value problem (5.15)–(5.18) was simulated using the same approach as the type A and type B models, and it was verified that it admits exploding solutions with the same explosion law (5.7).

6. Summary and concluding remarks

Thus, we have examined Couette flows with a free boundary in the limit $\varepsilon \rightarrow 1$, $\alpha = O(1)$ (where ε and α are given by (2.2)). For flows of types A and B (illustrated in figure 2), two boundary-value problems, (4.1), (3.30)–(3.33) and (4.2), (3.30)–(3.33), have been derived. In both cases, the global solution has been matched to the local solution (1.2)–(1.3) of Benney & Timson (1980). As a result, the parameters a and q of the latter have been determined: a has been related (by condition (3.36)) to the global solution, and the choice of q was restricted to the root of (1.3) such that $3/2 < q < 2$. The global boundary-value problem also determines the velocity V of the contact line.

Using the equations derived for Couette flows of type A, we found (for $\alpha \ll 1$ asymptotically, and for $\alpha \lesssim 0.1255$ numerically) steady solutions and showed (numerically) that they are stable. Flows of type B, in turn, were proved to never be steady.

Non-steady flows of both types have been examined through direct simulations of the asymptotic equations (4.1) and (4.2) with the boundary conditions (3.30)–(3.33). It was shown that, if no steady state exists, the solution evolves in such a way that the velocity of the contact line ‘explodes’, i.e. becomes infinite in a finite time (see (5.7)). Even though the ‘exploding’ solutions violate the applicability of the assumptions used, they are still self-consistent during the lead-up to the ‘explosion’. Thus, our results indicate a tendency to spontaneous acceleration of contact lines in Couette flows with a free boundary. This effect, as well as the existence of steady states for flows of type A, can be verified experimentally. Our approach can also be adapted for modelling the experiments with rolling drops (Richard & Quéré 1999; Reznik & Yarin 2002; Aussillous & Quéré 2004).

Note also that, in a ‘real’ hydrophobic liquid, the contact angle is never equal to 180° , but is rather close to this value. However, we still expect the present results to be asymptotically valid. Indeed, even though the pressure singularity is present in this case, the coefficient of the singular term in the solution is small (proportional to the sine of the contact angle; see Huh & Scriven (1971)). If this weak singularity is

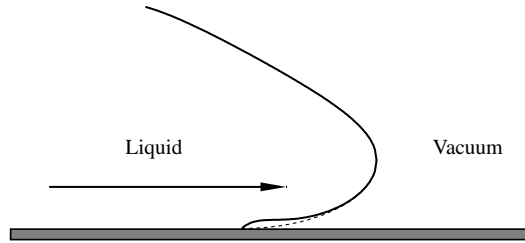


FIGURE 8. A flow over a plate (a schematic). The ‘microscopic’ contact angle differs significantly from 180° . The dotted line shows the ‘macroscopic’ structure of the free surface near the contact line.

‘removed’ by introducing the usual contact-line boundary layer, the effect on the global dynamics would be asymptotically negligible.

In fact, there are reasons to believe that, under certain conditions, the present results can be asymptotically valid even if the microscopic contact angle differs significantly from 180° . To illustrate this hypothesis, imagine a strong flow above a rigid plate. If the velocity of the flow is large enough, it should bend the free surface towards the plate (see the schematic in figure 8). This effectively means that the microscopic contact angle can only be observed in a small boundary layer near the contact line, whereas the macroscopic contact angle will be close to 180° . It can also be conjectured that, given a sufficiently strong flow, the same occurs with models that do not prescribe a microscopic contact angle, such as Shikhmurzaev’s (1993) interface formation theory. An investigation of these conjectures is now in progress.

Another possible extension of the present results is associated with the fact that both BT80 and the present work have neglected the gas surrounding the liquid, i.e. effectively replaced the gas with vacuum. If, however, the gas is taken into account, the approach of BT80 does not seem to work (which they mention themselves).

To understand the difference between liquid/vacuum and liquid/gas interfaces, note that a 180° contact angle for the liquid implies a 0° contact angle for the gas. As a result, the receding gas, just like any receding fluid with no slip and a contact angle other than 180° , leaves behind a thin film clinging to the substrate, so the advancing liquid flows on top of this film. Assuming that the film’s thickness scales with the product of the gas/liquid density ratio and the gas/liquid viscosity ratio, one can conjecture that this film is very thin. Then, the results of BT80 and ours can be viewed as the leading-order approximation of the ‘proper’ formulation, one including the gas.

We may also conjecture that, in most cases, the thin film of gas would rapidly dissolve in the surrounding liquid; still, it may cause a (microscopic) slip near the contact line. Thus, an accurate description of the near-contact-line gas film can help to develop a detailed mathematical model of the apparent slip of liquids on hydrophobic surfaces, which would be a useful addition to the existing physical ones (see Lauga & Brenner 2004).

There exists, however, at least one situation where the gas film trapped under the liquid does not dissolve: namely, the Leidenfrost effect (e.g. Bianco, Clanet & Quéré 2003; Bianco, Pirat & Ybert 2011). This would be another potential application of an extension of the present results to liquid/gas interfaces.

Acknowledgements

The authors are grateful to J. Chapman for a valuable comment. They also acknowledge the support of the Science Foundation Ireland (RFP Grant 11/RFP.1/MTH3281 and Mathematics Initiative Grant 06/MI/005).

Appendix A. Asymptotic solutions of (4.3)–(4.5)

A.1. The limit of small α

There are two asymptotic zones in this case, which will be referred to as zone 1 and zone 2. We also assume that

$$V = \frac{1}{2} + \alpha \hat{V}, \quad (\text{A } 1)$$

where \hat{V} is an order-one constant.

Zone 1 is described by the following variables:

$$X_1 = \frac{X}{\alpha^{3/2}}, \quad h_1 = h. \quad (\text{A } 2)$$

Substituting (A 1)–(A 2) into (4.3)–(4.4) and keeping the leading-order terms only, we obtain

$$\frac{d^3 h_1}{dX_1^3} + \frac{dh_1}{dX_1} = 0, \quad (\text{A } 3)$$

$$h_1 = 1, \quad \frac{dh_1}{dX_1} = 0 \quad \text{if } X_1 = 0, \quad (\text{A } 4)$$

hence,

$$h_1 = C + (1 - C) \cos X_1. \quad (\text{A } 5)$$

It turns out that (A 5) can be matched to its zone 2 counterpart only if

$$C = \frac{1}{2}, \quad (\text{A } 6)$$

in which case h_1 vanishes at $X_1 = \pi$, where

$$h_1 \sim \frac{(X_1 - \pi)^2}{4} \quad \text{as } X_1 \rightarrow \pi. \quad (\text{A } 7)$$

Zone 2, in turn, is described by

$$X_2 = \frac{X - \pi\alpha^{3/2}}{\alpha^2}, \quad h_2 = \frac{h}{\alpha}. \quad (\text{A } 8)$$

Substituting (A 1) and (A 8) into (4.3) and (4.5) and keeping the leading-order terms only, we obtain

$$\frac{h_2^3}{3} \frac{d^3 h_2}{dX_2^3} + \frac{1}{2} h_2 = -\hat{V}, \quad (\text{A } 9)$$

$$\frac{dh_2}{dX_2} \rightarrow 0 \quad \text{as } X_2 \rightarrow +\infty. \quad (\text{A } 10)$$

Using (A 8) and (A 2) to match $h_2(X_2)$ to the zone 1 asymptotics (A 7), we obtain

$$h_2 \sim \frac{1}{4} X_2^2 \quad \text{as } X_2 \rightarrow -\infty. \quad (\text{A } 11)$$

The boundary-value problem (A 9)–(A 11) differs from the famous Landau–Levich problem (Landau & Levich 1942; Wilson 1982; Benilov *et al.* 2010) only by coefficients. Thus, omitting technical details, we present the final result,

$$\hat{V} \approx -0.8426. \tag{A 12}$$

Together with formula (A 1), this expression describes the dependence of V on α in the limit $\alpha \rightarrow 0$ (it is represented by the sloping dotted line in figure 4).

A.2. *The limit of large α*

This limit will not be described in detail, as the expected solution is meaningless physically ($h > 1$ for some X). We present it here only for completeness.

There are three asymptotic zones in this case, denoted zone -1 , zone 0 and zone 1. The corresponding sets of variables are

$$X_{-1} = \frac{X}{\alpha}, \quad h_{-1} = h, \tag{A 13}$$

$$h_0 = \frac{h}{\alpha}, \quad X_0 = \frac{X}{\alpha^{3/2}}, \tag{A 14}$$

$$X_1 = \frac{X - 2\pi\alpha^{3/2}}{\alpha}, \quad h_1 = h, \tag{A 15}$$

for which the original boundary-value problem (4.3)–(4.5) yields

$$\frac{h_{-1}^3}{3} \frac{d^3 h_{-1}}{dX_{-1}^3} + (1 - V) h_{-1} = \frac{1}{2} - V + O(\alpha^{-1}), \tag{A 16}$$

$$h_{-1} = 1, \quad \frac{dh_{-1}}{dX_{-1}} = 0 \quad \text{if } X_{-1} = 0; \tag{A 17}$$

and

$$\frac{d^3 h_0}{dX_0^3} + \frac{dh_0}{dX_0} = O(\alpha^{-3/2}); \tag{A 18}$$

and

$$\frac{h_1^3}{3} \frac{d^3 h_1}{dX_1^3} + (1 - V) h_1 = \frac{1}{2} - V + O(\alpha^{-1}), \tag{A 19}$$

$$h_1 \rightarrow \frac{\frac{1}{2} - V}{1 - V} \quad \text{as } X_1 \rightarrow +\infty. \tag{A 20}$$

It can be shown that $h_0(X_0)$ can be matched to the solutions in the neighbouring zones only if

$$h_0 = \frac{A_0}{2} [1 + \cos(X_0 - \pi)] + B_0\alpha^{-1/2} \sin(X_0 - \pi) + C_0\alpha^{-1} + O(\alpha^{-3/2}), \tag{A 21}$$

where A_0 , B_0 and C_0 are order-one constants. Matching of (A 21) to h_{-1} and h_1 results in the following boundary conditions for zones -1 and 1,

$$h_{-1} \sim \frac{A_0}{4} X_{-1}^2 - B_0 X_{-1} + C_0 + O(\alpha^{-1}) \quad \text{as } X_{-1} \rightarrow +\infty, \tag{A 22}$$

$$h_1 \sim \frac{A_0}{4} X_1^2 - B_0 X_1 + C_0 + O(\alpha^{-1}) \quad \text{as } X_1 \rightarrow -\infty. \tag{A 23}$$

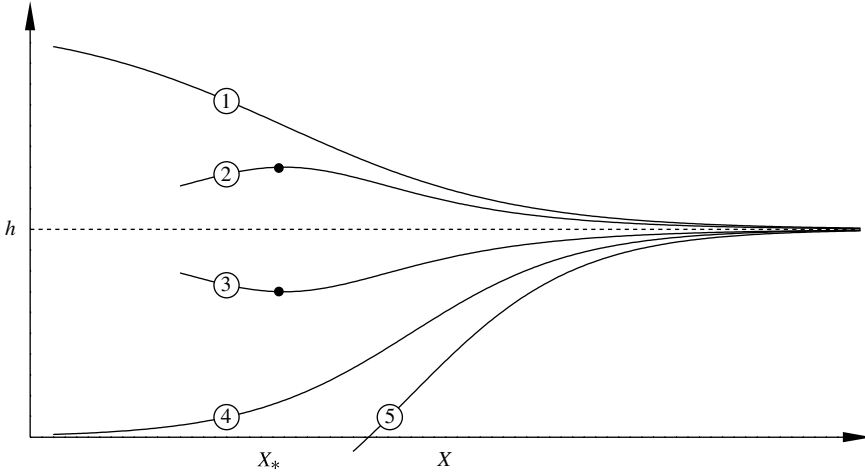


FIGURE 9. The five possible behaviours of the solution of the boundary-value problem (4.14) and (B 1). The dotted line indicates the limiting value of $h(X)$ as $X \rightarrow +\infty$ (see (B 1)). The black dots show the extrema (located at $X = X_*$) of curves 2 and 3.

The two coupled boundary-value problems, (A 16)–(A 17), (A 22) and (A 19)–(A 20), (A 23) determine A_0, B_0, C_0 and V . They have been solved numerically, yielding

$$V \approx 0.3275. \tag{A 24}$$

This value corresponds to the horizontal dotted line in figure 4.

Appendix B. The non-existence theorem for the boundary-value problem (4.19), (4.4)–(4.5)

Following the same approach as that used for deriving (4.17) and (4.12)–(4.13), one can show that (4.19), (4.5) imply that

$$h \rightarrow \frac{\frac{1}{2} - V}{1 - V} + A_1 e^{\lambda_1 X} \quad \text{as } X \rightarrow +\infty, \tag{B 1}$$

where A_1 is an undetermined constant and λ_1 satisfies

$$\alpha^3 \lambda^3 - \lambda + \frac{3(1 - V)^4}{(\frac{1}{2} - V)^3} = 0, \quad \text{Re } \lambda < 0. \tag{B 2}$$

Since $V \leq 1/2$ (otherwise the limiting value of h in (B 1) would be negative or larger than unity), one can show that (B 2) results in a unique real solution for λ . Thus, as $X \rightarrow +\infty$, the function $h(X)$ either monotonically grows or monotonically decays.

Then, there are five possible behaviours of $h(X)$ at finite X (see figure 9):

- (i) $h' < 0$ for all $X \in (-\infty, +\infty)$;
- (ii) $h' < 0$ for $X \in (X_*, +\infty)$ and $h'(X_*) = 0$, i.e. $X = X_*$ is a local maximum or an inflection point; the behaviour of h for $X < X_*$ is unimportant;
- (iii) $h' > 0, h > 0$ for $X \in (X_*, +\infty)$ and $h'(X_*) = 0$, i.e. $X = X_*$ is a local minimum or an inflection point; the behaviour of h for $X < X_*$ is unimportant;
- (iv) $h' > 0, h > 0$ for all $X \in (-\infty, +\infty)$;

(v) $h(X)$ crosses the X -axis and is negative somewhere.

Behaviours (i) and (iv) do not satisfy the boundary condition (4.4), whereas behaviour (v) makes the solution meaningless physically. Thus, to prove the non-existence theorem for the boundary-value problem (4.19), (4.4)–(4.5), it remains to eliminate behaviours (ii) and (iii).

To do so, divide (4.19) by $h^3/3$ and integrate it with respect to X over the interval $(X_*, +\infty)$, which yields

$$(\alpha^3 h'' - h)_{X \rightarrow +\infty} - (\alpha^3 h'' - h)_{X=X_*} = 3 \int_{X_*}^{+\infty} \left[\frac{1}{2} - V - (1 - V)h \right] \frac{1}{h^3} dX. \quad (\text{B } 3)$$

Re-arranging this identity using (B 1), we obtain

$$h(X_*) - \frac{\frac{1}{2} - V}{1 - V} - \alpha^3 h''(X_*) = 3(1 - V) \int_{X_*}^{+\infty} \left(\frac{\frac{1}{2} - V}{1 - V} - h \right) \frac{1}{h^3} dX. \quad (\text{B } 4)$$

Observe that behaviour (ii) implies that

$$h(X) - \frac{\frac{1}{2} - V}{1 - V} > 0 \quad \text{for } X \in (X_*, +\infty), \quad (\text{B } 5a)$$

$$h''(X_*) \leq 0. \quad (\text{B } 5b)$$

Thus, the left-hand (right-hand) side of equality (B 4) is positive (negative), which results in a contradiction and means that no solution exists.

Solutions with behaviour (iii) can be ruled out in the same manner as those with behaviour (ii).

REFERENCES

AUSSILLOUS, P. & QUÉRÉ, D. 2004 Shapes of rolling liquid drops. *J. Fluid Mech.* **512**, 133–151.
 BENOLOV, E. S. 2004 Explosive instability in a linear system with neutrally stable eigenmodes. Part 2: multi-dimensional disturbances. *J. Fluid Mech.* **501**, 105–124.
 BENOLOV, E. S., CHAPMAN, S. J., MCLEOD, J. B., OCKENDON, J. R. & ZUBKOV, V. S. 2010 On liquid films on an inclined plate. *J. Fluid Mech.* **663**, 53–69.
 BENOLOV, E. S., O'BRIEN, S. B. G. & SAZONOV, I. A. 2003 A new type of instability: explosive disturbances in a liquid film inside a rotating horizontal cylinder. *J. Fluid Mech.* **497**, 201–224.
 BENNEY, D. J. & TIMSON, W. J. 1980 The rolling motion of a viscous fluid on and off a rigid surface. *Stud. Appl. Maths* **63**, 93–98.
 BERTOZZI, A. L. & PUGH, M. 1996 The lubrication approximation for thin viscous films: regularity and long-time behaviour of weak solutions. *Commun. Pure Appl. Maths* **49**, 85–123.
 BERTOZZI, A. L. & PUGH, M. 2000 Finite-time blow-up of solutions of some long-wave unstable thin film equations. *Indiana Univ. Math. J.* **49**, 1323–1366.
 BIANCE, A.-L., CLANET, C. & QUÉRÉ, D. 2003 Leidenfrost drops. *Phys. Fluids* **15**, 1632–1637.
 BIANCE, A.-L., PIRAT, C. & YBERT, C. 2011 Drop fragmentation due to hole formation during Leidenfrost impact. *Phys. Fluids* **23**, 022104.
 DIDENKULOVA, I., PELINOVSKY, E., SOOMERE, T. & ZAHIBO, N. 2007 Runup of nonlinear asymmetric waves on a plane beach. In *Tsunami and Nonlinear Waves* (ed. A. Kundu). pp. 175–190. Springer.
 DUSSAN V., E. B. 1976 The moving contact line: the slip boundary condition. *J. Fluid Mech.* **77**, 665–684.
 DUSSAN V., E. B. & DAVIS, S. H. 1974 On the motion of a fluid–fluid interface along a solid surface. *J. Fluid Mech.* **65**, 71–95.

- FUJIMA, K. 2007 Tsunami runup in Lagrangian description. In *Tsunami and Nonlinear Waves* (ed. A. Kundu). pp. 191–208. Springer.
- HERVET, H. & DE GENNES, P.-G. 1984 The dynamics of wetting: precursor films in the wetting of ‘dry’ solids. *C. R. Acad. Sci., Ser. II: Mec., Phys., Chim., Sci. Terre Univers* **299**, 499–503.
- HOCKING, L. M. 1976 A moving fluid interface on a rough surface. *J. Fluid Mech.* **76**, 801–817.
- HOCKING, L. M. 1977 A moving fluid interface. Part 2. The removal of the force singularity by a slip flow. *J. Fluid Mech.* **79**, 209–229.
- HUH, C. & SCRIVEN, L. E. 1971 Hydrodynamic model of steady movement of a solid/liquid/fluid contact line. *J. Colloid Interface Sci.* **35**, 85–101.
- LANDAU, L. & LEVICH, B. 1942 Dragging of liquid by a plate. *Acta Physiochim. USSR* **17**, 42–54.
- LAUGA, E. & BRENNER, M. P. 2004 Dynamic mechanisms for apparent slip on hydrophobic surfaces. *Phys. Rev. E* **70**, 026311, 7 pages.
- MAHADEVAN, L. & POMEAU, Y. 1999 Rolling droplets. *Phys. Fluids* **11**, 2449–2453.
- MADSEN, P. A. & FUHRMAN, D. R. 2007 Analytical and numerical models for tsunami run-up. In *Tsunami and Nonlinear Waves* (ed. A. Kundu). pp. 209–236. Springer.
- MOFFATT, H. K. 1964 Viscous and resistive eddies near a sharp corner. *J. Fluid Mech.* **18**, 1–18.
- NGAN, C. G. & DUSSAN V., E. B. 1984 The moving contact line with a 180° advancing contact angle. *Phys. Fluids* **24**, 2785–2787.
- PISMEN, L. M. & NIR, A. 1982 Motion of a contact line. *Phys. Fluids* **25**, 3–7.
- REZNIK, S. N. & YARIN, A. L. 2002 Spreading of a viscous drop due to gravity and capillarity on a horizontal or an inclined dry wall. *Phys. Fluids* **14**, 911–925.
- RICHARD, D. & QUÉRÉ, D. 1999 Viscous drops rolling on a tilted non-wettable solid. *Europhys. Lett.* **48**, 286–291.
- SEPPECHER, P. 1996 Moving contact lines in the Cahn-Hilliard theory. *Intl J. Engng Sci.* **34**, 977–992.
- SHIKHMURZAEV, YU. D. 1993 The moving contact line on a smooth solid surface. *Intl J. Multiphase Flow* **19**, 589–610.
- TALANOV, V. I. 1964 Self-focusing of electromagnetic waves in nonlinear media. *Radiophys.* **8**, 254–257.
- THOMPSON, P. A. & TROIAN, S. M. 1997 A general boundary condition for liquid flow at solid surfaces. *Nature* **389**, 360–362.
- WAYNER, P. C. 1993 Spreading of a liquid film with a finite contact angle by the evaporation/condensation process. *Langmuir* **9**, 294–299.
- WEIDNER, D. E. & SCHWARTZ, L. W. 1994 Contact-line motion of shear-thinning liquids. *Phys. Fluids* **6**, 3535–3538.
- WILSON, S. D. R. 1982 The drag-out problem in film coating theory. *J. Engng Maths* **16**, 209–221.
- ZAKHAROV, V. E. 1972 Collapse of Langmuir waves. *Sov. Phys. JETP* **35**, 908–914.